Appendices

Appendix 1: Natural Maximum Analysis for RAC and HP Systems

The rate of heat input from low-temperature heat source to the heat pump is given by:

$$\dot{Q}_{\mathrm{E}} = \frac{Q_{\mathrm{E}}}{t_{\mathrm{E}}} = U_{\mathrm{E}} A_{\mathrm{E}} (\mathrm{LMTD})_{\mathrm{E}} = \dot{m}_{\mathrm{E}} C_{\mathrm{PE}} (T_{\mathrm{E1}} - T_{\mathrm{E2}}) \tag{A1.1}$$

Similarly, the rate of heat output from the heat pump to the heat sink is given by:

$$\dot{Q}_{\mathrm{C}} = \frac{Q_{\mathrm{C}}}{t_{\mathrm{C}}} = U_{\mathrm{C}} A_{\mathrm{C}} (\mathrm{LMTD})_{\mathrm{C}} = \dot{m}_{\mathrm{C}} C_{\mathrm{PC}} (T_{\mathrm{C2}} - T_{\mathrm{C1}}) \tag{A1.2}$$

where

$$(\mathrm{LMTD})_{\mathrm{E}} = \frac{(T_{\mathrm{E1}} - T_{\mathrm{e}}) - (T_{\mathrm{E2}} - T_{\mathrm{e}})}{\ln \dfrac{(T_{\mathrm{E1}} - T_{\mathrm{e}})}{(T_{\mathrm{E2}} - T_{\mathrm{e}})}} \quad \text{and}$$

$$(\mathrm{LMTD})_{\mathrm{C}} = \frac{(T_{\mathrm{c}} - T_{\mathrm{C1}}) - (T_{\mathrm{c}} - T_{\mathrm{C2}})}{\ln \dfrac{(T_{\mathrm{c}} - T_{\mathrm{C1}})}{(T_{\mathrm{c}} - T_{\mathrm{C2}})}}$$

Using LMTD expressions in Eqs. (A1.1) and (A1.2), we have:

$$T_{\mathrm{E2}} = T_{\mathrm{e}} + (T_{\mathrm{E1}} - T_{\mathrm{e}})\ \mathrm{e}^{-U_{\mathrm{E}} A_{\mathrm{E}} / \dot{m}_{\mathrm{E}} C_{\mathrm{PE}}} \tag{A1.3}$$

$$T_{\mathrm{C2}} = T_{\mathrm{c}} + (T_{\mathrm{c}} - T_{\mathrm{C1}})\ \mathrm{e}^{-U_{\mathrm{C}} A_{\mathrm{C}} / \dot{m}_{\mathrm{C}} C_{\mathrm{PC}}} \tag{A1.4}$$

Using Eqs. (A1.1), (A1.2), (A1.3), and (A1.4), we have:

S.C. Kaushik et al., *Finite Time Thermodynamics of Power and Refrigeration Cycles*,
https://doi.org/10.1007/978-3-319-62812-7

$$Q_{\mathrm{E}} = EE(T_{\mathrm{E1}} - T_{\mathrm{e}})t_{\mathrm{E}} \tag{A1.5}$$

$$Q_{\mathrm{C}} = CE(T_{\mathrm{c}} - T_{\mathrm{C1}})t_{\mathrm{C}} \tag{A1.6}$$

where

$$CE = C_{\mathrm{E}}\varepsilon_{\mathrm{E}}, \quad C_{\mathrm{E}} = \dot{m}_{\mathrm{E}} C_{\mathrm{PE}}, \quad C_{\mathrm{C}} = \dot{m}_{\mathrm{C}} C_{\mathrm{PC}},$$
$$\varepsilon_{\mathrm{E}} = 1 - \mathrm{e}^{-U_{\mathrm{E}} A_{\mathrm{E}}/\dot{m}_{\mathrm{E}} C_{\mathrm{PE}}}, \quad \text{and} \quad \varepsilon_{\mathrm{C}} = 1 - \mathrm{e}^{-U_{\mathrm{C}} A_{\mathrm{C}}/\dot{m}_{\mathrm{C}} C_{\mathrm{PC}}}$$

Now the total cycle time becomes:

$$t = \frac{Q_{\mathrm{E}}}{EE(T_{\mathrm{E1}} - T_{\mathrm{e}})} + \frac{Q_{\mathrm{C}}}{CE(T_{\mathrm{c}} - T_{\mathrm{C1}})} \tag{A1.7}$$

According to second law of thermodynamics:

$$\frac{\dot{Q}_{\mathrm{E}}}{T_{\mathrm{e}}} = \frac{\dot{Q}_{\mathrm{C}}}{T_{\mathrm{c}}} \tag{A1.8}$$

Equation (A1.8) gives:

$$T_{\mathrm{e}} = \frac{EE\,T_{\mathrm{E1}}\,T_{\mathrm{c}}}{EE\,T_{\mathrm{c}} + CE\,T_{\mathrm{c}} - CE\,T_{\mathrm{C1}}} \tag{A1.9}$$

Power input to heat pump system:

$$P = CE(T_{\mathrm{c}} - T_{\mathrm{C1}}) - \frac{CE\,EE\,(T_{\mathrm{c}} - T_{\mathrm{C1}})\,T_{\mathrm{E1}}}{(CE + EE)\,T_{\mathrm{c}} - CE\,T_{\mathrm{C1}}} \tag{A1.10}$$

For fixed T_{C1} and T_{E1}, power input is the function of refrigerant temperature T_{c} only. Minimizing power with respect to T_{c}, $\frac{\mathrm{d}P}{\mathrm{d}T_{\mathrm{c}}} = 0$, gives:

$$(T_{\mathrm{c}})_{\mathrm{O}} = \frac{\left(CE\sqrt{T_{\mathrm{C1}}} + EE\sqrt{T_{\mathrm{E1}}}\right)}{(CE + EE)}\sqrt{T_{\mathrm{C1}}} \tag{A1.11}$$

$$(T_{\mathrm{e}})_{\mathrm{O}} = \frac{\left(CE\sqrt{T_{\mathrm{C1}}} + EE\sqrt{T_{\mathrm{E1}}}\right)}{(CE + EE)}\sqrt{T_{\mathrm{E1}}} \tag{A1.12}$$

For numerical appreciation, let us assume:

$$T_{\mathrm{E1}} = 5^{\circ}\mathrm{C} = 278\mathrm{K}, T_{\mathrm{C1}} = 25^{\circ}\mathrm{C} = 298\mathrm{K}, C_{\mathrm{C}} = C_{\mathrm{E}} = 1.00\,\mathrm{kW/K},$$
$$\varepsilon_{\mathrm{C}} = \varepsilon_{\mathrm{E}} = 0.75\ \mathrm{kW/K}$$

Using these above typical values, Eqs. (A1.11) and (A1.12) give:

$$(T_{\mathrm{c}})_{\mathrm{O}} = 292.91\ \mathrm{K}, \quad (T_{\mathrm{e}})_{\mathrm{O}} = 282.91\,\mathrm{K}$$

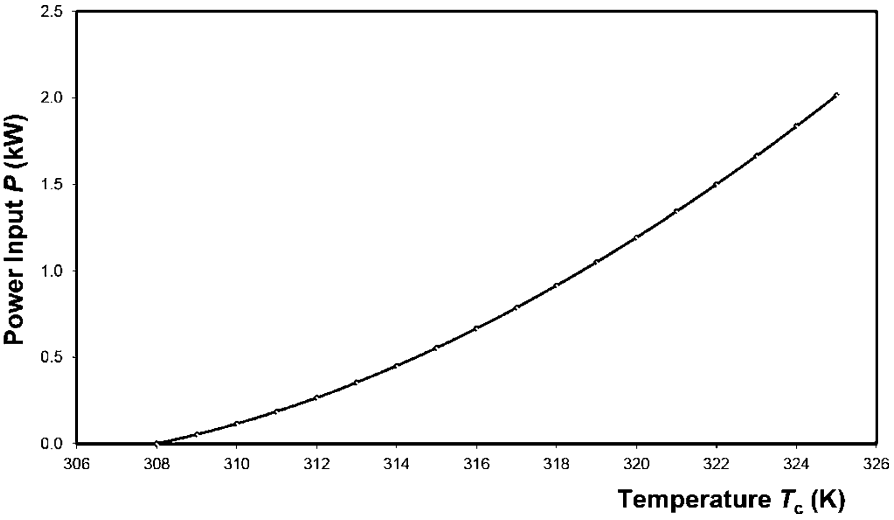

Fig. A1.1 Power input versus refrigerant temperature in condenser

These typical calculations show that $(T_e)_O$ is greater than T_{E1} and $(T_c)_O$ is less than T_{C1}, which is unrealistic. This result shows that these straightforward calculations do not work for a heat pump. A graph between power input (P) to the heat pump system and refrigerant temperature (T_c) is shown in Fig. A1.1, which indicates that power input is a monotonic increasing function of refrigerant temperature (T_c).

Similar results can be obtained for refrigeration/airconditioning systems. Thus, it is seen that there is no 'natural maximum' in case of R/AC and HP systems. Therefore, we have to use alternative method (Lagrangian multiplier method) for seeking the minimum input power (P) for a given desired output (viz. cooling load, heating load) for these systems.

Appendix 2: Optimization Method: Lagrangian Multiplier Method

To extremalize a function ψ_K subject to certain conditions or constraints ϕ_K, Lagrangian's undetermined multiplier method can be used in which each conditional function ϕ_K is multiplied by a multiplier λ_K, and the $\lambda_K\phi_K$ is added to the objective function ψ_K to define Lagrangian operator. Partial differentiation of the Lagrangian operator with respect to the variable parameters is taken and the extremal value of the variable parameters equated to zero. Now after substituting these extremal values in objective function, we can find optimal objective function (Band et al. 1982; Tolle 1975):

1. The method of Lagrangian multipliers gives a set of necessary conditions to identify optimal points of equality constrained optimization problems.
2. This is done by converting a constrained problem to an equivalent unconstrained problem with the help of certain unspecified parameters known as Lagrangian multipliers.

For example, the classical problem formulation:

Minimize $f(x_1, x_2, x_3,.....x_n)$
Subject to $h_1(x_1, x_2, x_3,..... x_n) = 0$

can be converted to minimize $L(x, v) = f(x) - v\, h_1(x)$
where $L(x, v)$ is the Lagrangian function and 'v' is an unspecified positive or negative constant called the Lagrangian multiplier.

Finding an Optimum Using Lagrangian Multipliers

1. Suppose that we fix $v = v_0$ and the unconstrained minimum of $L(x, v)$ occurs at $x = x^*$ and x^* satisfies $h_1(x^*) = 0$, then x^* minimizes $f(x)$ subject to $h_1(x) = 0$.
2. Trick is to find appropriate value for Lagrangian multiplier v.
3. This can be done by treating v as a variable, finding the unconstrained minimum of $L(x, v)$, and adjusting v so that $h_1(x) = 0$ is satisfied.

Typical Approach

1. Take derivative of $L(x, v)$ with respect to x_i and set them equal to zero.
2. If there are n variables, you will get n equations with $n + 1$ unknowns.
3. Express all x_i in terms of Lagrangian multiplier v.
4. Plug x in terms of v in constraint $h_1(x) = 0$ and solve v.
5. Calculate x by using the just found value for v.
6. Note that the n derivatives and one constraint equation result in $n + 1$ equations.

Appendix 3: Comparative Study of RAC and HP Systems Alternatively and Continuously Connected to Thermal Reservoirs

The refrigeration/airconditioning and heat pump systems alternatively as well as continuously connected to the thermal reservoirs (through external heating and cooling fluids) are analysed, in Chap. 7, and found the analytical expressions of optimal performance for both cases (Kumar, 2002).

The coefficient of performance for alternatively connected case is having similar form of the COP as that of continuously connected case but slightly differs because of different form of 'K' which depends on effectiveness, heat capacitance rates, and internal irreversibility. In order to have a numerical appreciation of the theoretical analysis for alternatively and continuously connected case, we have studied the effect of various input parameters on optimal working fluid temperatures, power input, and optimal coefficient of performance. The optimal coefficient of performance of refrigeration/airconditioning and heat pump systems and results are shown in Tables A3.1, A3.2, A3.3, A3.4, A3.5, A3.6, A3.7, A3.8, A3.9, A3.10, A3.11, A3.12, A3.13, and A3.14. For refrigeration/airconditioning system, during the variation of any one parameter, all other parameters are assumed to be constant as given below:

$$T_{\mathrm{Cl}} = 318\,\mathrm{K} \quad T_{\mathrm{El}} = 275\,\mathrm{K} \quad C_{\mathrm{C}} = C_{\mathrm{E}} = 1.00\,\mathrm{kW/K}$$
$$\varepsilon_{\mathrm{C}} = \varepsilon_{\mathrm{E}} = 0.75 \quad R_{\Delta S} = 1.0 \quad \text{and} \quad \mathrm{P_L} = 3.0\,\mathrm{kW}$$

For heat pump system, during the variation of any one parameter, all other parameters are assumed to be constant as given below:

$$T_{\mathrm{Cl}} = 310\,\mathrm{K} \quad T_{\mathrm{El}} = 283\,\mathrm{K} \quad C_{\mathrm{C}} = C_{\mathrm{E}} = 1.00\,\mathrm{kW/K}$$
$$\varepsilon_{\mathrm{C}} = \varepsilon_{\mathrm{E}} = 0.75 \quad R_{\Delta S} = 1.0 \quad \text{and} \quad \mathrm{P_H} = 3.0\,\mathrm{kW}$$

It can be seen from Tables A3.1, A3.2, A3.3, A3.4, A3.5, A3.6, A3.7, A3.8, A3.9, A3.10, A3.11, A3.12, A3.13, and A3.14 that coefficient of performance for continuously connected case is slightly higher than the corresponding COP for alternatively connected case. However, Tables A3.7 and A3.14 show that the difference in COP decreases as the internal irreversibility increases (value of $R_{\Delta S}$ decreases).

Table A3.1 Effect of heat source inlet fluid temperature on working fluid temperatures, power input, and performance of heat pump system in alternatively and continuously connected cases

T_{E1}	Alternatively connected				Continuously connected			
K	$(T_e)_o$ K	$(T_c)_o$ K	$\mathrm{COP_o}$	P_{in} kW	$(T_e)_o$ K	$(T_c)_o$ K	$\mathrm{COP_o}$	P_{in} kW
278	271.18	318.00	6.79	0.44	274.50	314.00	7.95	0.38
279	272.15	318.00	6.94	0.43	275.49	314.00	8.15	0.37
280	273.13	318.00	7.09	0.42	276.48	314.00	8.37	0.36
281	274.10	318.00	7.24	0.41	277.47	314.00	8.59	0.35
282	275.08	318.00	7.41	0.40	278.45	314.00	8.83	0.34
283	276.06	318.00	7.58	0.40	279.44	314.00	9.09	0.33
284	277.03	318.00	7.76	0.39	280.43	314.00	9.35	0.32
285	278.01	318.00	7.95	0.38	281.42	314.00	9.64	0.31
286	278.98	318.00	8.15	0.37	282.40	314.00	9.94	0.30
287	279.96	318.00	8.36	0.36	283.39	314.00	10.26	0.29

Table A3.2 Effect of heat sink inlet fluid temperature on working fluid temperatures, power input, and performance of heat pump system in alternatively and continuously connected cases

T_{C1}	Alternatively connected				Continuously connected			
K	$(T_e)_o$ K	$(T_c)_o$ K	COP_o	P_{in} kW	$(T_e)_o$ K	$(T_c)_o$ K	COP_o	P_{in} kW
300	275.84	308	9.58	0.31	279.32	304	12.32	0.24
302	275.88	310	9.09	0.33	279.35	306	11.48	0.26
304	275.93	312	8.65	0.35	279.37	308	10.76	0.28
306	275.97	314	8.26	0.36	279.39	310	10.13	0.3
308	276.01	316	7.90	0.38	279.42	312	9.58	0.31
310	276.06	318	7.58	0.40	279.44	314	9.09	0.33
312	276.10	320	7.29	0.41	279.46	316	8.65	0.35
314	276.14	322	7.02	0.43	279.48	318	8.26	0.36
316	276.18	324	6.78	0.44	279.51	320	7.90	0.38
318	276.22	326	6.55	0.46	279.53	322	7.58	0.40

Table A3.3 Effect of heat capacitance of heat source fluid on working fluid temperatures, power input, and performance of heat pump system in alternatively and continuously connected cases

C_C	Alternatively connected				Continuously connected			
kW/K	$(T_e)_o$ K	$(T_c)_o$ K	COP_o	P_{in} kW	$(T_e)_o$ K	$(T_c)_o$ K	COP_o	P_{in} kW
0.60	275.16	321.83	6.90	0.44	279.47	316.67	8.51	0.35
0.70	275.45	320.50	7.12	0.42	279.46	315.71	8.71	0.34
0.80	275.69	319.47	7.30	0.41	279.45	315.00	8.86	0.34
0.90	275.89	318.66	7.45	0.40	279.45	314.44	8.98	0.33
1.00	276.06	318.00	7.58	0.40	279.44	314.00	9.09	0.33
1.10	276.20	317.45	7.70	0.39	279.44	313.64	9.17	0.33
1.20	276.33	316.98	7.80	0.38	279.43	313.33	9.24	0.32
1.30	276.44	316.59	7.89	0.38	279.43	313.08	9.30	0.32
1.40	276.55	316.24	7.97	0.38	279.43	312.86	9.36	0.32
1.50	276.64	315.93	8.04	0.37	279.43	312.67	9.41	0.32

Table A3.4 Effect of heat capacitance of heat sink fluid on working fluid temperatures, power input, and performance of heat pump system in alternatively and continuously connected cases

C_E	Alternatively connected				Continuously connected			
kW/K	$(T_e)_o$ K	$(T_c)_o$ K	COP_o	P_{in} kW	$(T_e)_o$ K	$(T_c)_o$ K	COP_o	P_{in} kW
0.60	272.88	319.16	6.90	0.44	277.12	314.00	8.51	0.35
0.70	273.98	318.78	7.12	0.42	277.94	314.00	8.71	0.34
0.80	274.83	318.47	7.30	0.41	278.56	314.00	8.86	0.34
0.90	275.50	318.22	7.45	0.40	279.05	314.00	8.98	0.33
1.00	276.06	318.00	7.58	0.40	279.44	314.00	9.09	0.33
1.10	276.52	317.81	7.70	0.39	279.76	314.00	9.17	0.33
1.20	276.91	317.65	7.80	0.38	280.03	314.00	9.24	0.32
1.30	277.25	317.51	7.89	0.38	280.25	314.00	9.30	0.32
1.40	277.55	317.38	7.97	0.38	280.45	314.00	9.36	0.32
1.50	277.81	317.27	8.04	0.37	280.62	314.00	9.41	0.32

Table A3.5 Effect of effectiveness of sink side heat exchanger on working fluid temperatures, power input, and performance of heat pump system in alternatively and continuously connected cases

ε_C	Alternatively connected				Continuously connected			
–	$(T_e)_o$ K	$(T_c)_o$ K	COP_o	P_{in} kW	$(T_e)_o$ K	$(T_c)_o$ K	COP_o	P_{in} kW
0.20	273.35	332.75	5.60	0.54	279.56	325.00	7.15	0.42
0.30	274.32	326.32	6.28	0.48	279.51	320.00	7.90	0.38
0.40	274.93	322.98	6.72	0.45	279.48	317.50	8.35	0.36
0.50	275.36	320.90	7.05	0.43	279.46	316.00	8.65	0.35
0.60	275.69	319.47	7.30	0.41	279.45	315.00	8.86	0.34
0.70	275.95	318.43	7.50	0.40	279.44	314.29	9.02	0.33
0.75	276.06	318.00	7.58	0.40	279.44	314.00	9.09	0.33
0.80	276.15	317.62	7.66	0.39	279.44	313.75	9.14	0.33
0.90	276.33	316.98	7.80	0.38	279.43	313.33	9.24	0.32
1.00	276.48	316.46	7.91	0.38	279.43	313.00	9.32	0.32

Table A3.6 Effect of effectiveness of source side heat exchanger on working fluid temperatures, power input, and performance of heat pump system in alternatively and continuously connected cases

ε_E	Alternatively connected				Continuously connected			
–	$(T_e)_o$ K	$(T_c)_o$ K	COP_o	P_{in} kW	$(T_e)_o$ K	$(T_c)_o$ K	COP_o	P_{in} kW
0.20	264.31	321.75	5.60	0.54	270.10	314.00	7.15	0.42
0.30	269.28	320.32	6.28	0.48	274.27	314.00	7.90	0.38
0.40	271.95	319.48	6.72	0.45	276.40	314.00	8.35	0.36
0.50	273.65	318.90	7.05	0.43	277.69	314.00	8.65	0.35
0.60	274.83	318.47	7.30	0.41	278.56	314.00	8.86	0.34
0.70	275.70	318.14	7.50	0.40	279.19	314.00	9.02	0.33
0.75	276.06	318.00	7.58	0.40	279.44	314.00	9.09	0.33
0.80	276.37	317.87	7.66	0.39	279.66	314.00	9.14	0.33
0.90	276.91	317.65	7.80	0.38	280.03	314.00	9.24	0.32
1.00	277.35	317.46	7.91	0.38	280.32	314.00	9.32	0.32

Appendix 4: Entropic Average Temperature and Internal Irreversibility Parameter for VCR Cycle

Figure A4.1 is a *T*–*s* diagram of a simple ideal vapour compression cycle, and its equivalent Carnot cycle is shown in Fig. A4.2. A simple ideal vapour compression cycle involves four sequential processes, namely, isobaric evaporation, isentropic compression, isobaric condensation, and isentropic expansion. In equivalent Carnot cycle, the above-mentioned isobaric evaporation and condensation processes become isothermal processes. It is assumed that at the end of the condensation, state point 3 is saturated liquid, and after evaporation, state point 1 is at saturated

Table A3.7 Effect of internal irreversibility parameter on working fluid temperatures, power input, and performance of heat pump system in alternatively and continuously connected cases

$R_{\Delta s}$	Alternatively connected				Continuously connected			
–	$(T_e)_o$ K	$(T_c)_o$ K	COP_o	P_{in} kW	$(T_e)_o$ K	$(T_c)_o$ K	COP_o	P_{in} kW
0.50	278.75	316.83	1.79	1.68	281.21	314.00	1.81	1.66
0.55	278.46	316.97	1.93	1.55	281.03	314.00	1.97	1.52
0.60	278.18	317.10	2.11	1.42	280.85	314.00	2.16	1.39
0.65	277.90	317.22	2.32	1.29	280.68	314.00	2.39	1.26
0.70	277.62	317.35	2.58	1.16	280.50	314.00	2.67	1.12
0.75	277.35	317.46	2.90	1.03	280.32	314.00	3.03	0.99
0.80	277.09	317.58	3.31	0.91	280.15	314.00	3.49	0.86
0.85	276.82	317.69	3.86	0.78	279.97	314.00	4.13	0.73
0.90	276.56	317.79	4.61	0.65	279.79	314.00	5.05	0.59
0.95	276.31	317.90	5.74	0.52	279.62	314.00	6.49	0.46
1.00	276.06	318.00	7.58	0.40	279.44	314.00	9.09	0.33

Table A3.8 Effect of heat sink inlet fluid temperature on working fluid temperatures, power input, and performance of refrigeration/airconditioning system in alternatively and continuously connected cases

T_{C1}	Alternatively connected				Continuously connected			
K	$(T_c)_o$ K	$(T_e)_o$ K	COP_o	P_{in} kW	$(T_e)_o$ K	$(T_c)_o$ K	COP_o	P_{in} kW
310	319.58	267.00	5.08	0.59	271.00	314.64	6.21	0.48
312	321.64	267.00	4.89	0.61	271.00	316.67	5.93	0.51
314	323.70	267.00	4.71	0.64	271.00	318.70	5.68	0.53
316	325.76	267.00	4.54	0.66	271.00	320.73	5.45	0.55
318	327.82	267.00	4.39	0.68	271.00	322.76	5.24	0.57
318	327.82	267.00	4.39	0.68	271.00	322.76	5.24	0.57
320	329.88	267.00	4.25	0.71	271.00	324.79	5.04	0.60
322	331.95	267.00	4.11	0.73	271.00	326.82	4.85	0.62
324	334.01	267.00	3.98	0.75	271.00	328.85	4.68	0.64
326	336.07	267.00	3.87	0.78	271.00	330.88	4.53	0.66
328	338.13	267.00	3.75	0.80	271.00	332.91	4.38	0.69

vapour. It can be seen from Fig. A4.1 that during condensation, temperature of state point 2′ is higher than condensation temperature, so first it will desuperheat to state point 2, and then condensation will take place at constant temperature. For simplicity of theoretical analysis and to modify an ideal vapour compression cycle to an equivalent Carnot cycle to achieve the theoretical formula/analysis, we have used the concept of entropic average temperature with little loss of accuracy. Since the area under isobaric process 2′–2–3 in the *T*–*s* diagram of Fig. A4.1 represents the amount of heat rejection by VC cycle, we can make this area equal to the area under an isothermal process (2′–3) of Fig. A4.2 (a horizontal line), with an entropic

Table A3.9 Effect of heat source inlet fluid temperature on working fluid temperatures, power input, and performance of refrigeration/airconditioning system in alternatively and continuously connected cases

T_{E1}	Alternatively connected				Continuously connected			
K	$(T_c)_o$ K	$(T_e)_o$ K	COP_o	P_{in} kW	$(T_e)_o$ K	$(T_c)_o$ K	COP_o	P_{in} kW
265	328.22	257.00	3.61	0.83	261.00	322.95	4.21	0.71
267	328.14	259.00	3.75	0.80	263.00	322.91	4.39	0.68
269	328.06	261.00	3.89	0.77	265.00	322.87	4.58	0.66
271	327.98	263.00	4.05	0.74	267.00	322.84	4.78	0.63
273	327.90	265.00	4.21	0.71	269.00	322.80	5.00	0.60
275	327.82	267.00	4.39	0.68	271.00	322.76	5.24	0.57
277	327.75	269.00	4.58	0.66	273.00	322.73	5.49	0.55
279	327.67	271.00	4.78	0.63	275.00	322.69	5.77	0.52
281	327.60	273.00	5.00	0.60	277.00	322.66	6.07	0.49
283	327.53	275.00	5.24	0.57	279.00	322.63	6.40	0.47

Table A3.10 Effect of heat capacitance of heat sink fluid on working fluid temperatures, power input, and performance of refrigeration/airconditioning system in alternatively and continuously connected cases

C_C	Alternatively connected				Continuously connected			
kW/K	$(T_c)_o$ K	$(T_e)_o$ K	COP_o	P_{in} kW	$(T_e)_o$ K	$(T_c)_o$ K	COP_o	P_{in} kW
0.60	332.81	265.84	3.97	0.76	271.00	326.02	4.93	0.61
0.70	331.05	266.22	4.11	0.73	271.00	324.85	5.03	0.60
0.80	329.72	266.53	4.22	0.71	271.00	323.98	5.12	0.59
0.90	328.67	266.78	4.31	0.70	271.00	323.30	5.18	0.58
1.00	327.82	267.00	4.39	0.68	271.00	322.76	5.24	0.57
1.10	327.12	267.19	4.46	0.67	271.00	322.33	5.28	0.57
1.20	326.53	267.35	4.52	0.66	271.00	321.96	5.32	0.56
1.30	326.03	267.49	4.57	0.66	271.00	321.65	5.35	0.56
1.40	325.59	267.62	4.62	0.65	271.00	321.39	5.38	0.56
1.50	325.21	267.73	4.66	0.64	271.00	321.16	5.40	0.56

Table A3.11 Effect of heat capacitance of heat source fluid on working fluid temperatures, power input, and performance of refrigeration/airconditioning system in alternatively and continuously connected cases

C_E	Alternatively connected				Continuously connected			
kW/K	$(T_c)_o$ K	$(T_e)_o$ K	COP_o	P_{in} kW	$(T_e)_o$ K	$(T_c)_o$ K	COP_o	P_{in} kW
0.60	329.47	263.17	3.97	0.76	268.33	322.81	4.93	0.61
0.70	328.92	264.50	4.11	0.73	269.29	322.79	5.03	0.60
0.80	328.48	265.53	4.22	0.71	270.00	322.78	5.12	0.59
0.90	328.12	266.34	4.31	0.70	270.56	322.77	5.18	0.58
1.00	327.82	267.00	4.39	0.68	271.00	322.76	5.24	0.57
1.10	327.57	267.55	4.46	0.67	271.36	322.76	5.28	0.57
1.20	327.35	268.02	4.52	0.66	271.67	322.75	5.32	0.56
1.30	327.15	268.41	4.57	0.66	271.92	322.75	5.35	0.56
1.40	326.98	268.76	4.62	0.65	272.14	322.74	5.38	0.56
1.50	326.83	269.07	4.66	0.64	272.33	322.74	5.40	0.56

Table A3.12 Effect of effectiveness of sink side heat exchanger on working fluid temperatures, power input, and performance of refrigeration/airconditioning system in alternatively and continuously connected cases

ε_C	Alternatively connected				Continuously connected			
–	$(T_c)_o$ K	$(T_e)_o$ K	COP_o	P_{in} kW	$(T_e)_o$ K	$(T_c)_o$ K	COP_o	P_{in} kW
0.20	348.07	263.25	3.10	0.97	271.00	336.63	4.13	0.73
0.30	338.90	264.68	3.57	0.84	271.00	330.18	4.58	0.66
0.40	334.34	265.52	3.86	0.78	271.00	327.05	4.83	0.62
0.50	331.58	266.10	4.06	0.74	271.00	325.20	5.00	0.60
0.60	329.72	266.53	4.22	0.71	271.00	323.98	5.12	0.59
0.70	328.37	266.86	4.34	0.69	271.00	323.11	5.20	0.58
0.75	327.82	267.00	4.39	0.68	271.00	322.76	5.24	0.57
0.80	327.34	267.13	4.44	0.68	271.00	322.46	5.27	0.57
0.90	326.53	267.35	4.52	0.66	271.00	321.96	5.32	0.56
1.00	325.87	267.54	4.59	0.65	271.00	321.56	5.36	0.56

Table A3.13 Effect of effectiveness of source side heat exchanger on working fluid temperatures, power input, and performance of refrigeration/airconditioning system in alternatively and continuously connected cases

ε_E	Alternatively connected				Continuously connected			
–	$(T_c)_o$ K	$(T_e)_o$ K	COP_o	P_{in} kW	$(T_e)_o$ K	$(T_c)_o$ K	COP_o	P_{in} kW
0.20	333.53	252.25	3.10	0.97	260.00	322.97	4.13	0.73
0.30	331.22	258.68	3.57	0.84	265.00	322.87	4.58	0.66
0.40	329.93	262.02	3.86	0.78	267.50	322.83	4.83	0.62
0.50	329.09	264.10	4.06	0.74	269.00	322.80	5.00	0.60
0.60	328.48	265.53	4.22	0.71	270.00	322.78	5.12	0.59
0.70	328.02	266.57	4.34	0.69	270.71	322.77	5.20	0.58
0.75	327.82	267.00	4.39	0.68	271.00	322.76	5.24	0.57
0.80	327.65	267.38	4.44	0.68	271.25	322.76	5.27	0.57
0.90	327.35	268.02	4.52	0.66	271.67	322.75	5.32	0.56
1.00	327.09	268.54	4.59	0.65	272.00	322.75	5.36	0.56

Table A3.14 Effect of internal irreversibility parameter on working fluid temperatures, power input, and performance of refrigeration/airconditioning system in alternatively and continuously connected cases

$R_{\Delta s}$	Alternatively connected				Continuously connected			
–	$(T_c)_o$ K	$(T_e)_o$ K	COP_o	P_{in} kW	$(T_e)_o$ K	$(T_c)_o$ K	COP_o	P_{in} kW
0.50	335.26	265.34	0.65	4.58	271.00	327.67	0.71	4.25
0.55	333.92	265.61	0.78	3.86	271.00	326.77	0.84	3.58
0.60	332.81	265.84	0.92	3.26	271.00	326.02	0.99	3.02
0.65	331.87	266.04	1.09	2.76	271.00	325.39	1.18	2.54
0.70	331.05	266.22	1.29	2.33	271.00	324.85	1.40	2.14
0.75	330.34	266.38	1.53	1.96	271.00	324.38	1.68	1.79
0.80	329.72	266.53	1.83	1.64	271.00	323.98	2.02	1.48
0.85	329.16	266.66	2.21	1.36	271.00	323.62	2.47	1.21
0.90	328.67	266.78	2.71	1.11	271.00	323.30	3.07	0.98
0.95	328.22	266.90	3.40	0.88	271.00	323.02	3.93	0.76
1.00	327.82	267.00	4.39	0.68	271.00	322.76	5.24	0.57

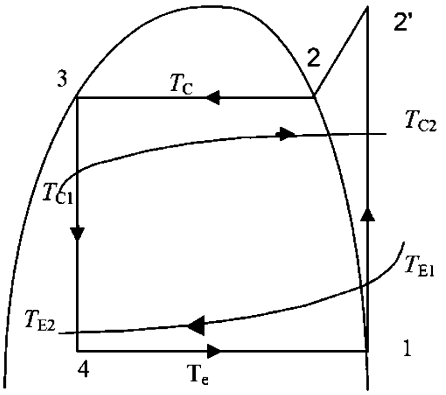

Fig. A4.1 *T–s* diagram of ideal vapour compression refrigeration/heat pump cycle

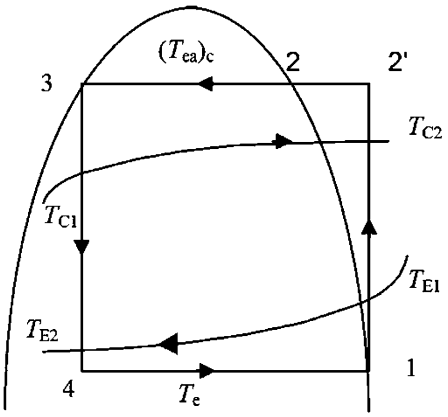

Fig. A4.2 *T–s* diagram of equivalent Carnot refrigeration/heat pump cycle

average temperature of heat rejection. The entropic average temperature T_{ea} can be defined as follows:

$$T_{ea} = \frac{\delta Q}{\Delta s}$$

where δQ and Δs are, respectively, the heat transfer and change in entropy from state point $2'$ to 3.

Entropic Average Temperature (Considering Isentropic Compression)

From the above equation and considering refrigeration/heat pump cycle 1–2′–2–3–4 (with isentropic compression) in Fig. A4.1, the entropic average temperature of heat rejection becomes:

$$(T_{ea})_c = \frac{h_2' - h_3}{s_2' - s_3}$$

Thus, for refrigerants (viz. R-12 and R-134a) after calculating entropy and enthalpy values at various state points, entropic average temperatures are calculated and tabulated in Tables A4.1 and A4.2. A sample calculation of entropic average temperature for R-12 is given below:

Let us consider, $T_c = 40\ ^\circ\text{C} = 313\ \text{K}$, $T_e = 10\ ^\circ\text{C} = 283\ \text{K}$.

Using computerized thermodynamic refrigerant tables (Sonntag et al. 1998) and considering Fig. A4.1:

$$P_c = P(T_c) = 0.9607\ \text{MPa}, \qquad P_e = P(T_e) = 0.4233\ \text{MPa}$$
$$h_3 = h_f(T_c) = 74.59\ \text{kJ/kg}$$
$$h_2 = h_g(T_c) = 203.2\ \text{kJ/kg}$$
$$s_3 = s_f(T_c) = 0.2718\ \text{kJ/kg-K}$$
$$s_2 = s_g(T_c) = 0.6825\ \text{kJ/kg-K}$$
$$s_1 = s_g(T_e) = s_2' = 0.6921\ \text{kJ/kg-K}$$
$$h_f(T_e) = 45.37\ \text{kJ/kg}$$
$$h_1 = h_g(T_e) = 191.7\ \text{kJ/kg}$$
$$s_f(T_e) = 0.1752\ \text{kJ/kg-K}$$
$$h_2' = 206.2\ \text{kJ/kg}$$

Entropic average temperature is given by $(T_{ea})_c = \left(h_2' - h_3\right)/\left(s_2' - s_3\right)$; now, on substituting the values of enthalpy and entropy, we have:

$$(T_{ea})_c = 40.13^\circ\text{C} = 313.13\text{K}, \quad (T_{ea})_e = T_e = 10.0^\circ\text{C} = 283\text{K}$$

Thus it is found that entropic average temperature [$(T_{ea})_c = 313.13$ K] is very close to the condensation temperature [$T_c = 313.0$ K], whereas entropic average

Table A4.1 Effect of condensation temperature on entropic average temperature with isentropic compression for R-12

T_c (K)	T_e (K)	$(T_{ea})_c$ (K)
313	283	313.1
315	283	315.2
317	283	317.3
319	283	319.2
321	283	321.4

Table A4.2 Effect of condensation temperature on entropic average temperature with isentropic compression for R-134a

T_c (K)	T_e (K)	$(T_{ea})_c$ (K)
313	283	313.0
315	283	315.3
317	283	317.2
319	283	319.3
321	283	321.3

temperature on evaporation side is same as evaporation temperature as no superheating has been assumed in the evaporator. Similarly, entropic average temperature for R-12 and R-134a with varying condensation temperature is calculated and tabulated below.

It can be seen from Tables A4.1 and A4.2 that entropic average temperatures are quite close to the condensation temperature, and it is only about 0.1% higher than the corresponding condensation temperature. So, the assumption of entropic average temperature as equivalent to condensation temperature simplifies the analysis considerably with little loss of accuracy.

Entropic Average Temperature (Considering Non-isentropic Compression)

If internal irreversibility due to friction, non-isentropic expansion/compression is accounted for the refrigeration/heat pump system, then the two isentropic processes become adiabatic processes with entropy generations which are shown by dotted lines (1–2″ and 3–4′) in Fig. A4.3.

On *T*–*s* diagram, the four processes of such a refrigeration/heat pump cycle constitute the cycle 1–2″–2–3–4′ as shown in Fig. A4.3. Now, entropic average temperature becomes:

$$(T_{ea})_c = \frac{h_2'' - h_3}{s_2'' - s_3}$$

With the help of this entropic average temperature, an isobaric process 2″–2′–2–3 of irreversible cycle (Fig. A4.3) can be replaced by an isothermal process 2″–2′–2–3 as shown in equivalent cycle (Fig. A4.4). A sample calculation of the entropic

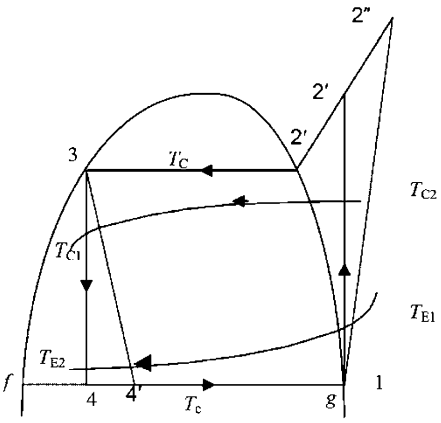

Fig. A4.3 *T*–*s* diagram of vapour compression refrigeration/heat pump cycle with non-isentropic compression and expansion

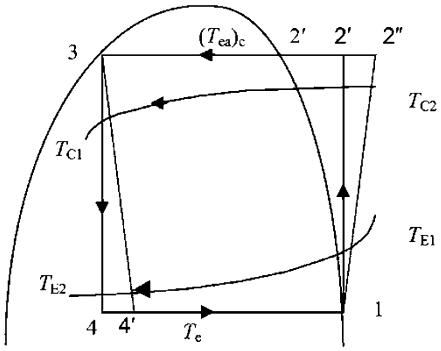

Fig. A4.4 *T–s* diagram of equivalent refrigeration/heat pump cycle with non-isentropic compression and expansion

average temperature of heat rejection with non-isentropic compression/expansion for R-12 is given below:

Let us consider, $T_c = 40\ ^\circ\text{C} = 313\ \text{K}, \quad T_e = 10\ ^\circ\text{C} = 283\ \text{K}$.

Following earlier Sect. 4.1 and considering Fig. A4.3:

$$h_1 = h_g(T_e) = 191.7\ \text{kJ/kg} = 206.2\ \text{kJ/kg}$$

Isentropic compression efficiency may be given as:

$$\eta_c = \frac{h_2' - h_1}{h_2'' - h_1}$$

Let, $\eta_c = 0.7$:

$$h_2'' \quad 212.41\ \text{kJ/kg}$$
$$s_2'' = 0.7113\ \text{kJ/kg}$$

Entropic average temperature in non-isentropic case is given by $(T_{ea})_c = \dfrac{h_2'' - h_3}{s_2'' - s_3}$.

On substituting the values of enthalpy and entropy, we have:

$$(T_{ea})_c = 40.59^\circ\text{C} = 313.6\ \text{K}, \quad (T_{ea})_e = T_e = 10.0^\circ\text{C} = 283\ \text{K}$$

Entropic average temperature with varying condensation temperature and compression efficiency for R-12 and R-134a are calculated and tabulated below.

Tables A4.3, A4.4, A4.5, and A4.6 show that entropic average temperature in case of non-isentropic compression is found to be slightly higher than the case of isentropic process, but it is still only 0.2% higher than the corresponding condensation temperature. So, entropic average temperature can be considered as equivalent to condensation temperature, for the sake of simplicity of theoretical analysis with a little loss of accuracy. Further, the condensation pressure has also been taken as discharge pressure with some loss of accuracy.

Table A4.3 Effect of condensation temperature on entropic average temperature with non-isentropic compression for R-12

T_c (K)	T_e (K)	h_c	$(T_{ea})_c$ (K)
313	283	0.90	313.2
315	283	0.90	315.3
317	283	0.90	317.3
319	283	0.90	319.3
321	283	0.90	321.4

Table A4.4 Effect of compression efficiency on entropic average temperature with non-isentropic compression for R-12

T_c (K)	T_e (K)	h_c	$(T_{ea})_c$ (K)
313	283	0.70	313.6
313	283	0.75	313.4
313	283	0.80	313.4
313	283	0.85	313.3
313	283	0.90	313.2

Table A4.5 Effect of condensation temperature on entropic average temperature with non-isentropic compression for R-134a

T_c (K)	T_e (K)	h_c	$(T_{ea})_c$ (K)
313	283	0.90	312.7
315	283	0.90	313.5
317	283	0.90	317.3
319	283	0.90	319.7
321	283	0.90	321.2

Table A4.6 Effect of compression efficiency on entropic average temperature with non-isentropic compression for R-134a

T_c (K)	T_e (K)	h_c	$(T_{ea})_c$ (K)
313	283	0.70	313.2
313	283	0.75	313.4
313	283	0.80	312.9
313	283	0.85	313.3
313	283	0.90	312.7

Internal Irreversibility Parameter

Considering Fig. A4.4, heat absorbed by reversible cycle (process 4–1), $Q_E = T_e(S_1 - S_4)$ and heat absorbed by irreversible cycle (process 4′–1), $Q'_E = T_e\left(S_1 - S'_4\right)$. Since $S_4 < S'_4$, so $Q'_E < Q_E$ (primes are added to quantities associated with the irreversible cycle). One can define an irreversible heat absorption parameter C_1, such that:

$$Q'_E = C_1 Q_E \quad \text{with} \quad C_1 = \frac{\left(s_1 - s'_4\right)}{\left(s_1 - s_4\right)} < 1 \tag{A4.1}$$

Similarly, an irreversible heat rejection parameter C_2 may be defined as:

$$Q'_c = C_2 Q_c \quad \text{with} \quad C_2 = \frac{(s''_2 - s_3)}{(s'_2 - s_3)} > 1 \tag{A4.2}$$

Assuming that the irreversible cycle operates between the same source and sink temperatures and that the effective thermal conductance remains the same, the second law requires: $\int \frac{dQ}{T} = \frac{Q'_E}{T_e} - \frac{Q'_c}{T_c} < 0$.

We can write the above inequality as:

$$\frac{Q'_c}{T_e} = R_{\Delta s} \frac{Q'_c}{T_c} \tag{A4.3}$$

where

$$R_{\Delta s} = \frac{C_1}{C_2} = \frac{s_1 - s'_4}{s''_2 - s_3} \tag{A4.4}$$

Thus, it is seen that internal irreversibility parameter $R_{\Delta S}$ represents the ratio of entropy differences and it can be calculated for any refrigerant, by calculating these entropy values at various state points of the cycle. A set of sample calculation of internal irreversibility for R-12 is given below.

Let us consider, $T_c = 40\ ^\circ\text{C} = 313\ \text{K} \quad T_e = 10\ ^\circ\text{C} = 283\ \text{K}$

Internal irreversibility parameter is calculated, using computerized thermodynamic refrigerant tables (Sonntag et al. 1998) and considering Figs. A4.3 and A4.4:

$$h_3 = h_f(T_c) = 74.59\,\text{kJ/kg}$$
$$s_3 = s_f(T_c) = 0.2718\,\text{kJ/kg-K}$$
$$s_1 = s_g(T_e) = 0.6921\,\text{kJ/kg-K}$$
$$h_f(T_e) = 45.37\,\text{kJ/kg}$$
$$h_1 = h_g(T_e) = 191.7\text{kJ/kg}$$
$$s_f(T_e) = 0.1752\,\text{kJ/kg-K}$$

Since expansion process is isenthalpic process, therefore:

$$h'_4 = h_3 = 74.59\,\text{kJ/kg}$$
$$h'_4 = h_f(T_e) + x'_4 h_{fg}(T_e)$$
$$x'_4 = 0.1997$$
$$s'_4 = s_f(T_e) + x'_4 S_{fg}(T_e)$$
$$s'_4 = 0.2784\,\text{kJ/kg-K}$$

In Sect. 4.2, it is seen with $h_c = 0.7$, $s_2'' = 0.7113\,\text{kJ/kg}$

$$R_{\Delta s} = \frac{s_1 - s_4'}{s_2'' - s_3}$$

On substituting the entropy values, we have:

$$R_{\Delta s} = 0.9413$$

Similar calculations have been carried out with varying compression efficiency and condensation temperature for R-12 and R-134a, and corresponding internal irreversibility parameters are calculated and tabulated below.

It can be seen clearly from Tables A4.7, A4.8, A4.9, and A4.10 that for both refrigerants (viz. R-12 and R-134a), internal irreversibility parameter increases and

Table A4.7 Effect of compression efficiency on internal irreversibility parameter for R-12

T_c (K)	T_e (K)	h_C	$R_{\Delta S}$
313	283	0.70	0.9413
313	283	0.75	0.9503
313	283	0.80	0.9587
313	283	0.85	0.9661
313	283	0.90	0.9727

Table A4.8 Effect of condensation temperature on internal irreversibility parameter for R-12

T_c (K)	T_e (K)	h_C	$R_{\Delta S}$
313	283	0.90	0.9727
315	283	0.90	0.9696
317	283	0.90	0.9660
319	283	0.90	0.9630
321	283	0.90	0.9590

Table A4.9 Effect of compression efficiency on internal irreversibility parameter for R-134a

T_c (K)	T_e (K)	h_C	$R_{\Delta S}$
313	283	0.70	0.9385
313	283	0.75	0.9487
313	283	0.80	0.9556
313	283	0.85	0.9644
313	283	0.90	0.9698

Table A4.10 Effect of condensation temperature on internal irreversibility parameter for R-134a

T_c (K)	T_e (K)	h_C	$R_{\Delta S}$
313	283	0.90	0.9698
315	283	0.90	0.9626
317	283	0.90	0.9645
319	283	0.90	0.9619
321	283	0.90	0.9561

approaches unity (endoreversible) with increasing compression efficiency/condensation temperature. For most practical cases, it will be between 0.94 and 0.97.

Appendix 5: Entropic Average Temperature and Internal Irreversibility Parameter for Modified VCR Cycle

Entropic Average Temperature for Irreversible VC R/AC and HP System with Liquid–Vapour Heat Exchanger

A sample calculation of entropic average temperature of heat rejection/evaporation for R-12 is given below.

Let us consider, $T_c = 40\ ^\circ\text{C} = 313\ \text{K}, \quad T_e = 10\ ^\circ\text{C} = 283\ \text{K}.$

Considering Fig. 7.5b and using computerized thermodynamic refrigerant tables (Sanntag et al. 1998):

$$\begin{aligned}
P_c &= P(T_c) = 0.9607\ \text{MPa}\\
P_e &= P(T_e) = 0.4233\ \text{MPa}\\
h_3 &= h_f(T_c) = 74.59\ \text{kJ/kg}\\
s_3 &= s_f(T_c) = 0.2718\ \text{kJ/kg-K}\\
s_1 &= s_g(T_e) = 0.6921\ \text{kJ/kg-K}\\
h_f(T_e) &= 45.37\ \text{kJ/kg}\\
h_1 &= h_g(T_e) = 191.7\ \text{kJ/kg}\\
s_f(T_e) &= 0.1752\ \text{kJ/kg-K}
\end{aligned}$$

Specific heat of saturated vapour of R-12 refrigerant (Prasad 1989) is given by:

$$C_{pg}(T) = 0.624 + 0.00319T + 3.353T^2 10^{-5}$$

Effectiveness of liquid–vapour heat exchanger may be defined as:

$$\varepsilon = \frac{\text{actual heat transfer}}{\text{maximum possible heat transfer}} \varepsilon = \frac{h_3 - h_3'}{C_{\min}(T_3 - T_1)} C_{\min} = C_{pg}(T = 10^\circ\text{C})$$

$$= 0.659253\,\text{kJ/kg-K}$$

Let us take $\varepsilon = 0.9$:

$$\begin{aligned}
h_3' &= 56.79\,\text{kJ/kg}\\
s_3' &= 0.2142\,\text{kJ/kg-K}
\end{aligned}$$

Effectiveness of L–V heat exchanger may also be written as:

$$\varepsilon = \frac{h_1' - h_1}{C_{\min}(T_3 - T_1)}$$
$$h_1' = 209.5\,\text{kJ/kg}$$
$$s_1' = 0.752\,\text{kJ/kg-K}$$
$$s_2' = s_1' = 0.752\,\text{kJ/kg-K}$$
$$h_2' = 226.0\,\text{kJ/kg}$$
$$h_4' = h_3' = 56.79\,\text{kJ/kg}$$
$$h_4' = h_f(T_e) + x_4' hfg(T_e)$$
$$x_4' = 0.0780427$$
$$s_4' = s_f(T_e) + x_4' sfg(T_e)$$
$$s_4' = 0.2155\,\text{kJ/kg-K}$$

Entropic average temperature on rejection side considering isentropic compression is given as:

$(T_{ea})_c = \frac{h_2' - h_3'}{s_2' - s_3'}$. On substituting the values of enthalpy and entropy, we have:

$$(T_{ea})_c = 41.63^\circ\text{C} = 314.63\ \text{K}$$

And entropic average temperature on evaporation side is given as:

$$(T_{ea})_e = \frac{h_1' - h_4'}{s_1' - s_4'}$$
$$(T_{ea})_e = 11.66^\circ\text{C} \quad = \quad 284.66\ \text{K}$$

If non-isentropic compression is considered, entropic average temperature of evaporation will remain unchanged, whereas entropic average temperature of heat rejection becomes

$$(T_{ea})_c = \frac{h_2'' - h_3'}{s_2'' - s_3'}$$

Isentropic compression efficiency may be given as $\eta_c = \frac{h_2' - h_1'}{h_2'' - h_1'}$.

Let $\eta_c = 0.9$:

$$h_2'' = 227.83\,\text{kJ/kg}$$
$$s_2'' = 0.7573\,\text{kJ/kg-K}$$
$$(T_{ea})_c = 41.94^\circ\text{C} = 314.94\ \text{K}$$

Similarly, entropic average temperature of condensation and evaporation for R-12 and R-134a is calculated and tabulated in Tables A5.1, A5.2, and A5.3.

Table A5.1 Entropic average temperature and internal irreversibility parameter for R-12 and R-134a with varying condensation temperature

T_c	T_e			*R-12*			*R-134a*		
				$(T_{ea})_e$	$(T_{ea})_c$		$(T_{ea})_e$	$(T_{ea})_c$	
K	K	Effectiveness	h_C	K	K	$R_{\Delta S}$	K	K	$R_{\Delta S}$
313	283	0.90	0.90	284.66	314.94	0.9878	283.21	313.05	0.9751
315	283	0.90	0.90	284.81	317.07	0.9870	282.90	315.48	0.9741
317	283	0.90	0.90	285.07	319.29	0.9862	283.09	317.58	0.9714
319	283	0.90	0.90	285.27	321.49	0.9850	283.28	319.56	0.9680
321	283	0.90	0.90	285.48	323.76	0.9845	282.95	321.60	0.9653

Table A5.2 Entropic average temperature and internal irreversibility parameter for R-12 and R-134a with varying compression efficiency

T_c	T_e			*R-12*			*R-134a*		
				$(T_{ea})_e$	$(T_{ea})_c$		$(T_{ea})_e$	$(T_{ea})_c$	
K	K	Effectiveness	h_C	K	K	$R_{\Delta S}$	K	K	$R_{\Delta S}$
313	283	0.90	0.70	284.66	315.86	0.9612	283.21	313.82	0.9456
313	283	0.90	0.75	284.66	315.53	0.9689	283.21	313.38	0.9536
313	283	0.90	0.80	284.66	315.27	0.9757	283.21	313.32	0.9617
313	283	0.90	0.85	284.66	315.07	0.9820	283.21	313.05	0.9684
313	283	0.90	0.90	284.66	314.94	0.9878	283.21	313.05	0.9751

Table A5.3 Entropic average temperature and internal irreversibility parameter for R-12 and R-134a with varying effectiveness of L–V heat exchanger

T_c	T_e			R-12			R-134a		
				$(T_{ea})_e$	$(T_{ea})_c$		$(T_{ea})e$	$(T_{ea})_c$	
K	K	Effectiveness	h_C	K	K	$R_{\Delta S}$	K	K	$R_{\Delta S}$
313	283	0.70	0.90	284.15	314.52	0.9855	282.93	312.99	0.9740
313	283	0.75	0.90	284.24	314.69	0.9864	283.00	312.96	0.9743
313	283	0.80	0.90	284.39	314.73	0.9867	283.07	312.92	0.9745
313	283	0.85	0.90	284.53	314.84	0.9873	283.14	313.44	0.9765
313	283	0.90	0.90	284.66	314.94	0.9878	283.21	313.05	0.9751

Internal Irreversibility Parameter for Irreversible VC R/AC and HP System with Liquid–Vapour Heat Exchanger

Similar to Appendix 4, internal irreversibility parameter can also be calculated for the present case with liquid–vapour heat exchanger. A sample calculation for R-12 is given below.

Internal irreversibility parameter for a system with L–V heat exchanger can be defined (following Appendix 4) as:

$$\frac{S_1' S_4'}{S_2'' S_3'}$$

On substituting the entropy values, we have:

$$\mathbf{R_{\Delta S}} = 0.9878$$

With varying compression efficiency, effectiveness, and condensation temperature, similar calculations have been carried out for R-12 and R-134a, and corresponding internal irreversibility parameters are found out and tabulated below.

It can be seen from Tables A5.1, A5.2, and A5.3 that even with liquid–vapour heat exchanger within a VC R/AC system, entropic average temperature of heat rejection and of heat extraction is, respectively, quite close to the condensation and evaporation temperatures. It is found that in this case, it is slightly higher than the case without liquid–vapour heat exchanger, but still it is only about 1.0% higher than the corresponding condensation/evaporation temperature. So, with a little loss of accuracy, it can be considered as equal to condensation and evaporation temperature, for the sake of simplicity in theoretical analysis.

It is further seen from the results that with increasing compression efficiency and effectiveness of liquid–vapour heat exchanger, the internal irreversibility parameter for both cases (viz. R-12, and R-134a) increases and reaches towards endoreversible case (i.e. $R_{\Delta s} = 1$). But it is found to be decreasing with increasing condensation temperature for both R-12 and R-134a.

Appendix 6: Comparison of Predicted and Reported Experimental Performance

Vapour Compression Systems

In order to have a comparison of theoretical results with the available experimental performance data, a simple comparative study for same set of operating conditions is given below.

Internal irreversibility parameter for a vapour compression system can be given as (considering Fig. A4.3 of Appendix 4):

$$R_{\Delta s} = \frac{s_1 - s_4'}{s_2'' - s_3} \tag{A6.1}$$

A set of sample calculation of actual internal irreversibility parameter for commercial R-22 chiller (Chua et al. 1996) is given below:

Inlet condenser temperature $T_{C1} = 297.09$ K
Inlet evaporator temperature $T_{E1} = 281.02$ K

Thermal conductance of heat exchanger on evaporator side $EE = 0.608$ kW/K
Thermal conductance of heat exchanger on condenser side $CE = 0.840$ kW/K
Cooling load $P_L = 9.8$ kW
Heat rejection rate on condenser side $P_H = 13.8$ kW

Heat transfer rates on evaporator and condenser sides are given by:

$$P_L = EE(T_{E1} - T_e) \tag{A6.2}$$

$$P_H = CE(T_c - T_{C1}) \tag{A6.3}$$

Using Eqs. (A6.2) and (A6.3), we have evaporation and condensation temperature as given by:

$$T_e = T_{E1} - \frac{P_L}{EE} \tag{A6.4}$$

$$T_c = T_{C1} + \frac{P_H}{CE} \tag{A6.5}$$

Now, substituting input parameters in Eqs. (A6.4) and (A6.5), we have:

$$T_e = -8.10^{\circ}\text{C} \quad T_c = 40.52^{\circ}\text{C}$$

Heat extraction and rejection rates may also be written as:

$$P_L = \dot{m}_r(h_1 - h_4') \tag{A6.6}$$

$$P_H = \dot{m}_r(h_2'' - h_3) \tag{A6.7}$$

where $\dot{m}_r$ is mass flow rate of refrigerant. With an assumption that state point 1 (saturated vapour) and state point 3 (saturated liquid) are saturated states (see Fig. A4.3 of Appendix 4), enthalpy and entropy values at various points (following computerized refrigerant tables, Sanntag et al. 1998) are given by:

$$h_1 = h_g = 246.9 \text{ kJ/kg}$$
$$h_f = 35.19 \text{ kJ/kg}$$
$$h_3 = h_4' = 94.96 \text{ kJ/kg}$$
$$s_3 = 0.3438 \text{ kJ/kg-K}$$
$$s_1 = 0.9392 \text{ kJ/kg-K}$$
$$s_f = 0.1405 \text{ kJ/kg-K}$$

Using Eqs. (A6.6) and (A6.7), we have:

$$
\begin{aligned}
h_2'' &= 308.92\,\text{kJ/kg} \\
s_2'' &= 1.014\,\text{kJ/kg-K} \\
h_3 &= h_4' = 94.96\,\text{kJ/kg} \quad \text{gives} \\
x_4' &= 0.2823 \\
s_4' &= 0.3660\,\text{kJ/kg-K} \\
R_{\Delta s} &= \frac{s_1 - s_4'}{s_2'' - s_3} = 0.8552
\end{aligned}
$$

The coefficient of performance of a VCR system continuously connected to the heat source/sink thermal reservoirs (see Chap. 7) is given by:

$$
\text{COP} = \left(\frac{\frac{T_{\text{C1}}}{R_{\Delta S}}}{T_{\text{E1}} - \frac{P_{\text{i}}}{K}} - 1 \right)^{-1} \tag{A6.8}
$$

where

$$
K = \frac{CE\,EE\,R_{\Delta S}}{R_{\Delta S} CE + EE}
$$

Using Eq. (A6.8) performance is calculated which is found to be as COP = 2.62, (1/COP = 0.382). However, for the same input parameters, experimental value (Chua et al. 1996) is COP = 2.68, (1/COP = 0.373).

Our predicted performance is coming only about 2.4% lower than the experimental value which may be because of our calculated value of internal irreversibility parameter which may be lower than the actual value because of the simplifying assumption of taking saturated states at points 1 and 3. For different set of input parameters, internal irreversibility parameters are calculated, and corresponding predicted irreversible performance and experimental performance (Chua et al. 1996) from a commercial R-22 chiller are tabulated in Table A6.1.

It can be seen from Table A6.1 that for the same input parameters (viz. inlet external fluid temperatures of evaporator and condenser, cooling load, and thermal conductance on evaporator and condenser side), predicted performance in endoreversible case ($R_{\Delta S} = 1.0$) is quite higher than experimental value, as expected, and in actual irreversible case ($R_{\Delta S}$ has been calculated for actual given input data), performance predicted by finite time thermodynamic model (when system is continuously connected to thermal reservoirs) is found to be very close (maximum difference is about 5%) to the experimental performance as reported in Chua et al. (1996). Optimal input power and heat rejection rates are also found to be comparable with the experimental values. If an alternatively connected model is considered, the predicted performance is found to be much lower than the experimental performance.

Table A6.1 A comparison between measured performance of a commercial reciprocating R-22 chillers as reported in Chua et al. (1996) and the performance predicted by endoreversible ($R_{\Delta s} = 1.0$) and irreversible (actual calculated $R_{\Delta s}$) model

T_{C1}	T_{E1}	P_L	EE	CE	Predicted				Predicted				Experimental (data from Chua et al. 1996)		
K	K	kW	kW/K	kW/K	Endoreversible model				Irreversible model						
						P_H	P_o			P_H	P_o		P_H	P_o	
					$R_{\Delta s}$	kW	kW	$1/\text{COP}_o$	$R_{\Delta s}$	kW	kW	$1/\text{COP}_o$	kW	kW	$1/\text{COP}_o$
297.09	281.02	9.8	0.608	0.840	1.0	11.5	1.70	0.173	0.8553	13.5	3.75	0.382	13.8	3.66	0.373
296.89	283.00	10.5	0.622	0.884	1.0	12.3	1.76	0.168	0.8648	14.3	3.78	0.360	14.5	3.71	0.353
296.81	285.37	11.4	0.643	0.918	1.0	13.3	1.86	0.163	0.8834	15.1	3.70	0.325	15.3	3.81	0.336
296.94	286.96	11.7	0.639	0.905	1.0	13.6	1.89	0.161	0.8872	15.4	3.71	0.317	15.6	3.84	0.329
296.90	288.99	12.4	0.646	0.907	1.0	14.4	1.97	0.159	0.8981	16.1	3.70	0.299	16.3	3.90	0.315
296.88	291.00	12.9	0.649	0.917	1.0	14.9	2.00	0.155	0.9008	16.6	3.74	0.290	16.8	3.92	0.302
299.75	281.00	9.8	0.618	0.869	1.0	11.6	1.77	0.181	0.8634	13.5	3.70	0.377	13.7	3.74	0.380
299.75	283.00	10.5	0.640	0.900	1.0	12.3	1.85	0.176	0.8754	14.2	3.70	0.352	14.4	3.81	0.364
299.75	285.41	11.3	0.672	0.939	1.0	13.2	1.90	0.168	0.8798	15.1	3.80	0.336	15.3	3.94	0.348
299.67	287.00	11.9	0.689	0.953	1.0	13.9	1.96	0.165	0.8877	15.7	3.81	0.320	15.9	3.98	0.335
299.74	289.01	12.7	0.716	0.992	1.0	14.7	2.03	0.160	0.8915	16.6	3.92	0.309	16.8	4.10	0.322
299.67	290.99	13.4	0.734	1.007	1.0	15.5	2.08	0.155	0.8939	17.4	4.02	0.300	17.6	4.14	0.308

References

Andresen, B., Salamon, P. and Berry, R.S. (1984). Thermodynamics in finite time. *Physics Today*, **37**, 62–70.

Badescu, V. (1992). Optimum operation of solar convertor in combustion with a Stirling or Ericsson heat engine. *Energy*, **17**, 601–607.

Band, Y.B., Kafri, O. and Salamon, P. (1982). Finite time thermodynamics optimal expansion of a heated working fluid. *J. Appl. Phys*, **53(1)**, 8–28.

Bejan, A. (1982). Entropy generation through heat and fluid flow. John Wiley, New York, 181.

Bejan, A. (1993). Power and refrigeration plants for minimum heat exchanger inventory. *ASME, I. Energy Res. Tech*, **115**, 148–150.

Bejan, A. (1995). Theory of heat transfer-irreversible power plants-II. The optimal allocation of heat exchange equipment. *Int. J. Heat Mass Transfer*, **38(3)**, 433–444.

Bejan, A. (1996a). Models of power plants that generate minimum entropy while operating at maximum power. *American Journal of Physics*, **64(8)**, 1054–1059.

Bejan, A. (1996b). Entropy generation minimization: The new thermodynamics of finite-size devices and finite time processes. *J. Appl. Phys*, **79(3)** 1191–1215.

Berry, R.S., Kazakov, V., Sieniutycz, S., Szwast, Z. and Tsirlin, A.M. (1999). Thermodynamic optimization of finite-time processes. John Wiley & Sons, Ltd. ISBN 0 471 967521.

Bhardwaj, P.K., Kaushik, S.C. and Jain, S. (2001). Finite Time heat transfer and thermodynamic optimization of an irreversible Rankine cycle airconditioning system. Published in International Conference on "Emerging Technologies in Airconditioning and Refrigeration" organized by ISHRAE and ASHRAE in New Delhi, ACRECONF-2001 September 26–28, New Delhi, India, 398–408.

Bhardwaj, P.K. Kaushik, S.C. and Jain, S. (2003a). Finite Time Thermodynamic Optimization of an Irreversible Rankine Cycle Heat Pump System. *Indian Journal of Pure and Applied Physics*, **41**, 515–521.

Bhardwaj, P.K., Kaushik, S.C. and Jain, S. (2003b). Finite Time Optimization of an Endoreversible and Irreversible Vapour-Absorption Refrigeration System. *Energy Conversion and Management*, **44**, 1131–1144.

Bhardwaj, P.K., Kaushik, S.C. and Jain, S. (2003c). Finite Time Optimization of an Irreversible Vapour-Absorption Heat Pump System. *International Journal of Ambient Energy*, **24(4)**, 207–219.

Bhardwaj, P.K., Kaushik, S.C. and Jain, S. (2005). General Performance Characteristics of an Irreversible Vapour-Absorption Refrigeration System using Finite Time Thermodynamic Approach. *International Journal of Thermal Science*, **44(2)**, 189–196.

S.C. Kaushik et al., *Finite Time Thermodynamics of Power and Refrigeration Cycles*,
https://doi.org/10.1007/978-3-319-62812-7

Bhargava, R. and Peretto, A. (2002). A unique approach for thermo-economic optimization of an intercooled, reheat, and recuperated gas turbine for cogeneration applications. *J. Eng. for Gas Turbine & Power*, **124**, 881–891.

Blanchard, C.H. (1980). Coefficient of performance for finite speed heat pump. *J. Appl. Phys*, **51 (5)**, 2471–2472.

Blank, D.A., Davis, G.W. and Wu, C. (1994). Power optimization of an endoreversible Stirling cycle with regeneration. *Energy*, **19**, 125–133.

Blank, D.A. and Wu, C. (1995). Power optimization of an extra-terrestrial solar radiant Stirling heat engine, *Energy*, **20(6)**, 523–530.

Blank, D.A. and Wu, C. (1996a). Power limit of an endoreversible Ericsson cycle with regeneration. *Energy Convs. Mgmt*, **37**, 59–66.

Blank, D.A. and Wu, C. (1996b). Finite time power limit for solar-radiant Ericsson engines for space applications. *Applied Thermal Engineering*, **18**, 1347–1357.

Carnot, S. (1824). Reflections on the Motive Power of Fire. Bachelier, Paris.

Cengel, Y.A. and Boles, M.A. (2006). Thermodynamics. An Engineering approach. 5th edition. McGraw Hill.

Chambadal, P. (1957). Les centrales nuclearies. Paris: Armand Colin, 41–58.

Chen, J. (1994). The maximum power and maximum efficiency of an irreversible Carnot heat engine. *J. Phys. D: Appl. Phys*, **27**, 1144–1149.

Chen, J. (1995). The equivalent cycle system of an endoreversible absorption refrigerator and its general performance characteristics. *Energy*, **20(10)**, 995–1003.

Chen, J. and Andresen, B. (1995). Optimal analysis of primary performance parameters for an endoreversible absorption heat pump. *Heat Recovery System & CHP*, **15(8)**, 723–731.

Chen, J. (1997a). Optimal performance analysis of irreversible cycles used as heat pumps and refrigerators. *J. Phys. D: Appl. Phys*, **30**, 582–587.

Chen, J. (1997b). Effect of regenerative losses on the efficiency of Stirling heat engine at maximum power output. *Int. Journal of Ambient Energy*, **18**, 107–112.

Chen, J. (1998). Minimum power input of irreversible Stirling refrigerator for given cooling rate. *Energy Conv. & Mgmt*, **39(12)**, 1255–1263.

Chen, J. and Schouten, J.A. (1998). Optimum performance characteristic of an irreversible absorption refrigeration system. *Energy Conv. & Mgmt*, **39(10)**, 999–1007.

Chen, J. and Schouten, J.A. (1999). The comprehensive influence of several major irreversibilities on the performance of an Ericsson heat engine. *Applied Thermal Engineering*, **19**, 555.

Chen, J., Tyagi, S.K. and Wu, C. (2003). Optimal design on the performance parameters of an irreversible Carnot heat engine based on the thermoeconomic approach. *Int. Journal of Ambient Energy*, **24**, 201–206.

Chen, J. and Yan, Z. (1988). Optimal performance of an endoreversible-combined refrigeration cycle. *J. Appl. Phys*, **63(10)**, 4795–4798.

Chen, J. and Yan, Z. (1989). Unified description of endoreversible cycles. *Physical Review A*, **39 (8)**, 4140–4146.

Chen, J., Yan, Z., Chen, L. and Andresen, B. (1998). Efficiency bound of solar-driven Stirling heat engine system. *Int. Journal Energy Res*, **22**, 805–812.

Chen, L., Wu, C. and Sun, F. (1997). Optimal coefficient of performance and heating load relationship of three-heat-reservoir endoreversible heat pump. *Energy Conv. & Mgmt*. **38(8)**, 727–733.

Chen, L., Wu, C. and Sun, F. (1999a). Finite time thermodynamic optimization or entropy generation minimization of energy systems. *J. Non-Equilibrium Thermodynamics*, **24**, 327–359.

Chen, L., Wu, C., Sun, F. and Cao, S. (1999b). Maximum profit performance of a three-heat-reservoir heat pump. *Int. J. Energy Research*, **23**, 773–777.

Chen, L., Zheng, J., Sun, F. and Wu, C. (2001). Optimum distribution of heat exchanger inventory for power density optimization of an endoreversible closed Brayton cycle. *J. Phys. D: Appl. Phys*, **34**, 422–427.

Chen, W.Z., Sun, F.R., Cheng, S.M. and Chen, L.G. (1995). Study on optimal performance and working temperatures of endoreversible forward and reverse Carnot cycles. *Int. J. Energy Research*, **19**, 751–759.

Chua, H.T., Ng, K.C. and Gordon, J.M. (1996). Experimental study of the fundamental properties of reciprocating chillers and their relation to thermodynamic modeling and chiller design. *Int. J. Heat Mass Transfer*, **39(11)**, 2195–2204.

Curzon, F.L. and Ahlborn, B. (1975). Efficiency of a Carnot engine at maximum power output. *American Journal of Physics*, **43**, 22–24.

Davis, G.W. and Wu, C. (1997). Finite time analysis of a geothermal heat engine driven airconditioning system. *Energy Conv. & Mgmt*. **38(3)**, 263–268.

Erbay, L.B., Göktun, S. and Yavuz, H. (2001). Optimal design of the regenerative gas turbine engine with isothermal heat addition. *Applied Energy*, **68**, 249–269.

Erbay, L.B. and Yavuz, H. (1997). Analysis of Stirling heat engine at maximum power conditions. *Energy*, **22**, 645–650.

Goktun, S. (1997). Optimal performance of an irreversible refrigerator with three heat source (IRWTHS). *Energy*, **22(1)**, 27–31.

Goktun, S. and Ozkaynak, S. (1997). Optimum performance of a corrugated collector driven irreversible Carnot heat engine and absorption refrigerator. *Energy*, **22(5)**, 481–485.

Göktun, S. and Yavuz, H. (1999). Thermal efficiency of a regenerative Brayton cycle with isothermal heat addition. *Energy Conv. Mangt*, **40**, 1259–1266.

Hoffmann, K.H., Burzler, J.M. and Schubert, S. (1997). Endoreversible thermodynamics. *J Non-Equilib. Thermodynamics*, **22**, 311–355.

Holman, J.P. (1992). Heat Transfer 1963 (7th ed. in SI units, 1992). McGraw-Hill, ISBN 0-07-112644-9, 539–584.

Ibrahim, O.M., Klein, S.A. and Mitchell, J.W. (1991). Optimum heat power cycles for specified boundary conditions. *J. Engg. Gas Turbines Power*, **113**, 514–521.

Kaushik, S.C. (1999). State-of-the-art on finite time thermodynamics. Internal Report CES, IIT Delhi, India.

Kaushik, S.C., Singh, N. and Kumar, S. (1999a). Thermodynamic evaluation of a modified steam regenerative Brayton heat engine for solar thermal power generation. *Solar Energy Society of India*, **9**, 63–75.

Kaushik, S.C., Kumar, P. and Khaliq, A. (1999b). Analysis of a endoreversible Rankine Cycle Cooling System. *Energy Opportunities*, **xiv(1&2)**, 20–29.

Kaushik, S.C. and Kumar, S. (2000a). Finite time thermodynamic analysis of an endoreversibble Stirling heat engine with regenerative losses. *Energy*, **25**, 989–1003.

Kaushik, S.C. and Kumar, S. (2000b). Finite time thermodynamic evaluation of irreversible Ericsson and Stirling heat pump cycles, Proceedings of 4th Minsk International Seminar on Heat Pipes, Heat Pumps & Refrigerators, Minsk, Belarus 2000b, 113–126.

Kaushik, S.C., Kumar, P. and Jain, S. (2000). A Parametric Study based on Finite Time Thermodynamic Analysis of a Solar-Engine driven Airconditioning System. *SESI Journal*, **10(2)**, 63–78.

Kaushik, S.C., Kumar, P. and Jain, S. (2001). Finite Time Thermodynamic Optimisation of an Irreversible Heat Pump System Using the Lagrangian Multiplier Method. *International Journal of Ambient Energy*, **22(2)**, 105–112.

Kaushik, S.C. and Kumar, S. (2001). Finite time thermodynamic evaluation of irreversible Ericsson and Stirling heat engines. *Energy Convers. Mgmt*, **42**, 295–312.

Kaushik, S.C. and Tyagi, S.K. (2002). Finite time thermodynamic analysis of a nonisentropic regenerative Brayton heat engine. *Int. J. Solar Energy*, **22**, 141–151.

Kaushik, S.C., Tyagi, S.K., Bose, S.K. and Singhal, M.K. (2002a). Performance evaluation of irrerversible Ericsson and Stirling heat pump cycles. *Int. J. Thermal Sciences*, **41**, 193–200.

Kaushik, S.C., Kumar, P. and Jain, S. (2002b). Finite Time Optimization of Irreversible Airconditioning System Using Method of Lagrangian Multiplier *Journal of Energy and Environment* **2**, 53–61.

Kaushik, S.C., Kumar, P. and Jain, S. (2002c). Performance Evaluation of Irreversible Cascaded Refrigeration and Heat Pump Cycles. *Energy Conversion and Management*, **43(17)**, 2405–2424.

Kaushik, S.C., Bhardwaj, P.K. and Jain, S. (2002d). Finite Time Thermodynamics in Energy Conversion Processes. Published in National Conference on "Advances in Contemporary Physics and Energy-2002", Feb. 8–9, IIT Delhi, New Delhi, India, 464–486.

Kaushik, S.C., Tyagi, S.K. and Singhal, M.K. (2003). Parametric study of an irreversible regenerative Brayton heat engine with isothermal heat addition. *Energy Convers Mgmt*, **44**, 2013–2025.

Kays, W.M. and London, A.L. (1964). Compact heat exchangers. Second edition, McGraw-Hill, New York.

Kodal, A., Sahin, B., Ekmekei, I. and Yilmaz, T. (2003). Thermoeconomic optimization for irreversible absorption refrigerators and heat pumps. *Energy Convers. Mgmt*, **44**, 109–123.

Kodal, A., Sahin, B. and Erdil, A. (2002). Performance analysis of two-stage irreversible heat pump under maximum heating load per unit total cost conditions. *Exergy—An Int. Journal*, **2**, 159–166.

Kodal, A., Sahin, B. and Yilmaz, T. (2000). Effect of internal irreversibility and heat leakage on the finite time thermoeconomic performance of refrigerators and heat pumps, *Energy Conv. & Mgmt*, **41**, 607–619.

Kumar, S. (2000). Finite time thermodynamic analysis and second law evaluation of thermal energy conversion systems. Ph.D. Thesis, C.C.S. University, Meerut India.

Kumar, P. (2002). Finite time thermodynamic analysis of refrigeration airconditioning and heat pump systems. Ph.D. Thesis, CES, IIT Delhi, India.

Ladas, H.G. and Ibrahim, O.M. (1994). Finite time view of Stirling heat engine. *Energy*, **19**, 837–843.

Lee, W.Y. and Kim, S.S. (1992). Finite time optimization of a Rankine heat engine. *Energy Conv. & Mgmt*, **33(1)**, 59–67.

Leff, H.S. (1987). Thermal efficiency at maximum work output: New results for old heat engines. *American Journal of Physics*, **55(7)**, 602–610.

Leff, H.S. and Teeters, W.D. (1978). EER, COP and second law efficiency for airconditioner. *Am. J. Phys*, **41(1)**, 19–22.

Medina, A., Rocco, J.M.M. and Hernandez, C. (1996). Regenerative gas turbine at maximum power density conditions. *J. Phys. D: Appl. Phys*, **29**, 2802–2805.

Moran, M.J. and Shapiro, H.N. (eds.) (2007). Fundamentals of Engineering Thermodynamics. Wiley, New York.

Negri-di, M.G., Gambini, M. and Peretto, A. (1995). Reheat and regenerative gas turbine for feed water repowering of steam power plant. ASME Turbo Expo. Houston, June 5–8, 1995.

Novikov, I.I. (1957). The efficiency of atomic power stations (A review). *Attommaya Energia*, **3**, 409.

Prasad, M. (1989). Refrigeration and airconditioning data book. Wiley Eastern Limited, ISBN 81-224-0104-x.

Redcenco, V., Vargas, J.V.C. and Bejan, A. (1998). Theoretical optimization of a gas turbine power plant with pressure drop irreversibilities. *J. Energy Res. Tech*, **129**, 233–240.

Sahin, B., Kodal, A., Yilmaz, T. and Yavuz, H. (1996). Maximum power density analysis of irreversible Joule-Brayton engine. *J. Phys. D: Appl. Phys*, **29**, 1162–1167.

Sahin, B., Kodal, A. and Kaya, S.S. (1998). A comparative performance analysis of irreversible regenerative reheating Joule-Brayton heat engine under maximum power density and maximum power condition. *J. Phys D: Appl. Phys.* **31**, 2125–2131.

Sahin, B. and Kodal, A. (1999). Finite time thermoeconomic optimization for endoreversible refrigerators and heat pumps. *Energy Conv. & Mgmt*, **40**, 951–960.

Salamon, P. and Nitzan, A. (1981). Finite time optimizations of a Newton's law Carnot cycle. *J. Chem Phys*, **74(6)**, 3546–3560.

Senft, J.R. (1998). Theoretical limits on the performance of Stirling engine. *Int Journal Energy Res*, **22**, 991–1000.

Sonntag, R.E., Borgnakke, C. and Van Wylen, G.J. (1998). Fundamentals of thermodynamics. Fifth Edition. John Wiley & Sons Inc.

Tolle, H. (1975). Optimization methods. Springer, Berlin.

Trukhow, V.S., Tursunbaev, I.A., Lezhebokov, I.A. and Kenzhaev, I.G. (1997). Energy balance of autonomous solar power plant, with the Stirling engine *Appl Solar Energy*, **33**, 17–23.

Tyagi, S.K., Kaushik, S.C. and Tyagi, B.K. (2000). Thermodynamic analysis of a regenerative Brayton cycle with isothermal heat addition, NREC-2000, 419–424, Nov. 30-Dec. 2, 2000, IIT Bombay, India.

Tyagi, S.K., Kaushik, S.C. and Salhotra, R. (2002). Ecological optimization and parametric study of irreversible Ericsson and Stirling heat engines. *Journal of Phys D: Appl. Phys*, **35**, 2668–2675.

Tyagi, S.K., Chen, J. and Hua, B. (2004a). Performance evaluation and parametric study of irreversible Carnot heat pump and refrigerator cycles. Proceedings of 3rd International Symposium on Heat Transfer Enhancement and Energy Conservation, Guangzhou, China.

Tyagi, S.K., Chen, J. and Kaushik, S.C. (2004b). Thermoeconomic optimization and parametric study of an irreversible Stirling heat pump cycle. *Int. J. of Thermal Sciences*, **43**, 105–112.

Tyagi, S.K., Zhou, Y. and Chen, J. (2004c). Optimum criteria on the performance of an irreversible Braysson heat engine based on the new thermoeconomic approach. *Entropy—An Int. Journal*, **6**, 244–256.

Tyagi, S.K. and Kaushik, S.C. (2005). Ecological optimization of an irreversible regenerative intercooled Brayton heat engine with direct heat loss. *Int. Journal of Ambient Energy*, **26**, 81–92.

Tyagi, S.K., Chen, G.M., Wang, Q. and Kaushik, S.C. (2006a). A new thermoeconomic approach and parametric study of irreversible regenerative Brayton refrigeration cycle. *Int. Journal of Refrigeration*, **29**, 1167–1174.

Tyagi, S.K., Chen, G.M., Wang, Q. and Kaushik, S.C. (2006b). Thermodynamic analysis and parametric study of an irreversible regenerative-intercooled-reheat Brayton cycle heat engine Int. Journal of Thermal Sciences, **45**, 829–840.

Tyagi, S.K., Chen, J. and Kaushik, S.C. (2007). Effects of the intercooling on the performance of an irreversible regenerative modified Brayton cycle. *Int. Journal of Power and Energy Systems*, **27**, 56–64.

Tyagi, S.K., Wang, S.W. and Park, S.R. (2008). Performance criteria on different pressure ratios of an irreversible modified complex Brayton cycle. *Indian Journal of Pure & Applied Physics*, **46**, 565–574.

Tyagi, S.K. (2009). Effects of intercooling on the performance of a realistic regenerative Brayton heat engine cycle. *Int. Journal of Sustainable Energy*, **28**, 231–245.

Tyagi, S.K., Wang, Q., Xia, P. and Chen, G.M. (2010). Optimization of an irreversible Carnot refrigerator working between two heat reservoirs. *Int. Journal of Exergy*, **7**, 76–88.

Vecchiarelli, J., Kawall, J.G. and Wallace, J.S. (1997). Analysis of a concept for increasing the efficiency of a Brayton cycle via isothermal heat addition. *Int. Journal of Energy Research*, **21**, 113–127.

Wang, W., Chen, L., Sun, F. and Wu, C. (2003). Performance analysis of and irreversible variable temperature heat reservoir closed intercooled regenerated Brayton cycle. *Energy Convers Mgmt*, **44**, 2713–2732.

Wu, C. (1988). Power optimization of a finite time Carnot heat engine. *Energy*, **13(9)**, 681–687.

Wu, C. (1993a). Cooling capacity optimization of a waste heat absorption refrigeration cycle. *Heat Recovery Systems & CHP,* **13(2)**, 161–166.

Wu, C. (1993b). Maximum cooling load of a heat-engine driven refrigerator. *Energy Conv. & Mgmt*, **34(8)**, 691–696.

Wu, C. (1993c). Performance of a solar-engine driven airconditioning system. *Int. J. Ambient Energy*. **14(2)**, 77–82.

Wu, C. (1993d). Specific heating load of an endoreversible Carnot heat pump. *Int. J. Ambient Energy*. **14(1)**, 25–28.
Wu, C. (1995). Maximum obtainable specific cooling load of a refrigerator. *Energy Conv. & Mgmt*, **36(1)**, 7–10.
Wu, C., Chen, L. and Chen, J. (eds.), (1999). Recent advances in finite time thermodynamics. New York: Nova Science Publishing, 560.
Wu, C., Chen, L. and Sun, F. (1996). Performance of regenerative Brayton heat engine. *Energy*, **21**, 71–76.
Wu, C., Chen, L. and Sun, F. (1998a). Optimization of steady flow heat pumps. *Energy Conv. & Mgmt*, **39(5,6)**, 445–453.
Wu, C., Chen, L. and Sun, F. (1998b). Effect of heat transfer law on finite time exergoeconomic performance of Carnot heat pump. *Energy Conv. & Mgmt*, **39(7)**, 579–588.
Wu, C., Chen, L., Sun, F. and Cao, S. (1998c). Optimal collector temperature for solar driven heat pumps. *Energy Conv. & Mgmt*, **39(1–2)**, 143–147.
Wu, C. and Kiang, R.L. (1990). Work and power optimization of a finite time Brayton cycle. *Int. J. Ambient Energy*, **11**, 129–136.
Wu, C. and Kiang, R.L. (1991). Power performance of a nonisentropic Brayton cycle. *J. Engg. Gas Turbines Power*, **113**, 501–504.
Wu, C. and Kiang, R.L. (1992). Finite time thermodynamic analysis of a Carnot engine with internal irreversibility. *Energy*, **17(12)**, 1173–1178.
Yan, Z. and Chen, J. (1989). An optimal endoreversible three-heat-source refrigerator. *J. Appl. Phys*, **65(1)**, 1–4.
Zhou Y., Tyagi, S.K. and Chen, J. (2004). The optimal performance of an irreversible Braysson heat engine cycle, *Int. J. Therm. Sci*., **43**, 1101–1106.

Index

S.C. Kaushik et al., *Finite Time Thermodynamics of Power and Refrigeration Cycles*,
https://doi.org/10.1007/978-3-319-62812-7